Radio Science, Volume ???, Number , Pages 1–17,

Space-Time Ambiguity Function in 3-D ISR

John Swoboda,[1] Joshua Semeter,[1] Philip Erickson[2]

Corresponding author: J. P. Swoboda, Department of Electrical & Computer Engineering, Boston University, 8 Saint Marys Street Boston, MA 02215, USA. (swoboj@bu.edu)

[1]Department of Electrical & Computer Engineering, Boston University, Boston, Massachusetts, USA.

[2]Atmospheric Science Division, MIT Haystack Observatory, Westford Massachusetts, USA.

By leveraging electronically steerable phased array antenna technology, incoherent scatter radars (ISR) have now become full three-dimensional remote sensors for ionosphere plasmas. Currently these systems are operating in the high latitude region where the ionosphere is highly dynamic in both space and time. Because of the highly dynamic nature of the ionosphere in this region it is import to differentiate between artifacts and the true behavior of the plasma. Often the three dimension data is fitted in a spherical coordinate space and then the parameters are interpolated to a Cartesian grid. This and other sources of error could be impacting the reconstructions of the plasma parameters.

In this study we present a new way of analyzing 3-D dimension ISR through use of the space-time ambiguity function. This concept is similar to the range ambiguity function that is used in traditional ISR for scanning antenna systems but has been extended to all spatial dimension along with time as well.

The use of this new ambiguity function allow us to pose this problem in terms of a linear inverse problem for the lags of the intrinsic plasma autocorrelation function. From this we can explore the impact of non-stationarity in the plasma parameters in both time and space. Along with showing possible artifacts we will begin to explore ways of reducing these artifacts.

1. Introduction

Incoherent scatter radar (ISR) systems have enabled researchers since the 1950's to explore the ionosphere *Gordon* [1958]. Using methodology developed by Dougherty, Farley and others these systems can give measurements of electron density N_e, Ion temperature T_i, electron temperature T_e, Ion velocity V_i and other plasma parameters *Dougherty and Farley* [1960], *Farley et al.* [1961], *Hagfors* [1961], *Dougherty and Farley* [1963]. These parameters are measured by fitting a theoretic autocorrelation derived from first principles physics to an estimated intrapulse time autocorrelation of the scattered radar signal *Lehtinen and Huuskonen* [1996].

As with any real world measurement method there is a non-ideal ambiguity which gives these sensors a type of resolution. Often in ISR these ambiguities are only carried out over range and time. The range ambiguity is controlled by the pulse shape and the time ambiguity is controlled by the integration time.

A number techniques have been developed to reduce the impact of these ambiguities, two techniques often shown in the literate are full profile analysis or deconvolution methods. Full profile analysis consists of fitting value to the entire range gate of values *Holt et al.* [1992], *Lehtinen* [1989], *Lehtinen et al.* [1997], *Hysell et al.* [2008]. This technique often places constraints on the physical parameters, *Hysell et al.* [2008]. Because the the relationship between the autocorrelation function and the lags are non-linear this method often yields algorithms that require a large amount computation.

Deconvolution methods, such as in *Nikoukar et al.* [2008] treat the problem as a linear inverse problem of the lags. Method such as total-variations or Tikihonov regularization can be applied to the lags to try to fill in the missing information nation from the null space of the operator. These methods are easy to compute and can rely on a large body of knowledge from engineering communities that study linear inverse problems. The problem with these methods is researchers are unsure how to constrain the norms of the data or its derivatives.

Recently phase array technology has started to be leveraged by ISR community. The AMISR systems have already been deployed both at the Poker Flat Alaska and Resolute Bay Canada ami [2014]. The EISCAT-3D project is currently being developed using phased array technology as well and will be capable of multistatic processing eis [2005]. These new systems are already being used to create three dimensional reconstructions of plasma parameters *Semeter et al.* [2009], *Nicolls and Heinselman* [2007], *Dahlgren et al.* [2012a],*Dahlgren et al.* [2012b].

Even though these systems are already in use there is no formal derivation of a three dimensional ambiguity function for these systems. In a highly dynamic region like the high latitude ionosphere this lack of knowledge can be problematic. There are numerous phenomena such as polar cap patches that may be moving through the field of view at very high speeds *Dahlgren et al.* [2012a].

These three-dimensional reconstructions often consist of taking the fitted parameters and then interpolating them to a Cartesian space from the system's natural spherical coordinate space *Butler* [2013]. The step of fitting the autocorrelation

function to the theoretical functions to find the final plasma parameters is a non-linear operation. Because of this it is impossible to exactly predict the impact on the parameter values as different plasma populations move through the field of view of the radar. Alternatively it is possible to treat the formation of the autocorrelation estimates as a linear process with each lag as an independent channel *Nikoukar et al.* [2008].

In this publication we will develop a model for a full three dimensional space-time ambiguity function for 3-D ISR systems. This function can also be modified to show the ambiguity within the rest frame of the moving plasma. In the end this full three dimensional can be represented as kernel in a Fredholm integral equation like in Equation 1 with $f(s)$ being the lag of the autocorrelation function at a specific time and position.

$$g(t) = \int_a^b K(t,s) f(s) ds \tag{1}$$

The impact of the three-dimensional ambiguity on moving plasma will be shown through simulation. This ISR simulator fully emulates the ISR data creation process at the IQ level.

Lastly possible mitigation techniques will be explored. These mitigation techniques will borrow heavily from the image and signal processing literature.

2. Space-Time Ambiguity

In the ISR literature the measurement ambiguity along the range dimension is often referred to simply as the ambiguity function *Hysell et al.* [2008]. This only shows the measurement ambiguity along the range r. Due to the three-dimensional imaging capability of phased array ISR systems we will define a new set of terminology to describe this more complicated measurement which is now imaging the ionosphere in three-dimensional coordinates $\mathbf{r} = [x, y, z]^T$. We will represent the sampled coordinates within the radar with $_s$ such as $\mathbf{r}_s$.

Specifically we will refer to the measurement ambiguity in the range dimension as the range ambiguity, $W(r, r_s, \tau)$. The measurement ambiguity in the elevation and azimuth angles will be referred to as the angular or cross range ambiguity $F(\theta, \phi, \theta_s, \phi_s)$, where θ is the physical elevation angle, ϕ is the physical azimuth angle, θ_s is the elevation angle that the radar is pointing at and ϕ_s is the azimuth angle that the radar is pointing at. The since these two functions are separable they can be multiplied together to form the full spatial ambiguity $K(\tau, \mathbf{r}, \mathbf{r}_s)$. Lastly integration time for each measurement will be referred to the time ambiguity. Again like the full spatial ambiguity function we can multiply the space and time ambiguity functions to get the Space-Time ambiguity function which will be represented as $A(\tau, \mathbf{r}_s, \mathbf{r}, t_s, t)$.

2.1. Derivation

In order to develop the space-time ambiguity we will use two different sets of time commonly known in radar literature as fast-time n and slow-time t. Fast-time looks at time on the order of the radar systems A/D conversion while slow-time time is

looking at time on the order of the system's pulse repetition interval *Richards* [2005]. We will use the same reference for fast-time but slow time will be the time it takes the plasma to change state and thus change the ACF.

In order to start we will first develop the range ambiguity which is due to the pulse shape and receiver filter on the ISR systems. If we look at data received by the ISR system at time n, with a wavenumber $\mathbf{k}$ and pulse shape $s(n)$, noted as $x(n)$ we can see that the received signal can be represented as the following

$$x(n) \propto h(n) * \int_{\mathbf{r}} e^{-j\mathbf{k}\cdot\mathbf{r}} s(n - \frac{2r}{c}) n_e(\mathbf{r}, n) d\mathbf{r}, \tag{2}$$

where $h(n)$ is the receiver filter, $n_e(\mathbf{r}, n)$ is the electron density fluctuation. Generally it is assumed that the pass band of the filter is larger then the bandwidth of the electron density fluctuation *Kudeki* [2003]. As such it can be assumed that filter will only act on the the shape of the pulse. This will change Equation 2 to the following:

$$x(n) \propto * \int_{\mathbf{r}} e^{-j\mathbf{k}\cdot\mathbf{r}} a(n - \frac{2r}{c}) n_e(\mathbf{r}, n) d\mathbf{r} \tag{3}$$

where $a(n) = h(n) * s(n)$.

When the autocorrelation of the signal is done we find the following formula, *Nikoukar et al.* [2008].

$$\langle x(n) x^*(n+\tau) \rangle = \int_{\mathbf{r}'} \int_{\mathbf{r}} e^{-2j\mathbf{k}\cdot(\mathbf{r}'-\mathbf{r})} a(n - \frac{2r}{c}) a^*(n+\tau - \frac{2r'}{c}) \langle n_e(\mathbf{r}, n) n_e(\mathbf{r}', n+\tau) \rangle d\mathbf{r} d\mathbf{r}' \tag{4}$$

where r' is the magnitude of the vector $\mathbf{r}'$. We can make some simplifying assumption at this point that the space-time autocorrelation function of $n_e(\mathbf{r},t)$, $\langle n_e(\mathbf{r},n)n_e(\mathbf{r}',n+\tau)\rangle$, will vanish as the magnitude of $\mathbf{x}\equiv\mathbf{r}'-\mathbf{r}$ increases. Once the spatial correlation is removed we can rewrite Equation 4 as

$$\langle x(n)x^*(n+\tau)\rangle = \int_{\mathbf{r}} a(n-\frac{2r}{c})a^*(n+\tau-\frac{2r}{c})\int_{\mathbf{x}} e^{-2j\mathbf{k}\cdot\mathbf{x}}\langle n_e(\mathbf{r},n)n_e(\mathbf{x}+\mathbf{r},n+\tau)\rangle d\mathbf{x}d\mathbf{r}. \tag{5}$$

The inner integral is a spatial Fourier transform evaluated at the wave number of the radar $\mathbf{k}$

$$\langle |n_e(\mathbf{k},r,\tau)|^2\rangle \equiv \int_{\mathbf{x}} e^{-2j\mathbf{k}\cdot\mathbf{x}}\langle n_e(\mathbf{r},b)n_e(\mathbf{x}+\mathbf{r},n+\tau)\rangle d\mathbf{x}. \tag{6}$$

Equation 5 becomes

$$\langle x(n)x^*(n+\tau)\rangle = \int_{r} a(n-\frac{2r}{c})a^*(n+\tau-\frac{2r}{c})\langle |n_e(\tau,\mathbf{k},\mathbf{r})|^2\rangle dr. \tag{7}$$

It should be noted that the term $a(n)a^*(n+\tau)$ is the soft target ambiguity function. If n is replaced with $2r_s/c$ we can see that the this function represented as $W(\tau,r_s,r)$ *Nikoukar* [2010]. In order to simplify notation we will represent $\langle |n_e(\tau,\mathbf{k},\mathbf{r})|^2\rangle$, as $R(\tau,\mathbf{r})$. Assuming, for the moment, that R only varies across the range dimension r we can now represent this in the form of a Fredholm integral equation

$$\langle x(2r_s/c)x^*(2r_s/c+\tau)\rangle = \int_{r} W(\tau,r_s,r)R(\tau,r)dr. \tag{8}$$

This function is in a way a lag dependent smoothing along the range dimension of $R(\tau, r)$.

The spatial ambiguity across angle is determined by the antenna beam pattern. In phase array radars this beam pattern is ideally the array factor multiplied by the element pattern *Balanis* [2005]. The array factor is determined by a number of things including the element spacing in both x and y (dx, dy) and the wave number of the radar, k. Making idealized assumptions with no mutual coupling and that the array elements are cross dipole elements AMISR systems will have the following array pattern for pointing angle (θ_s, ϕ_s),

$$F(\theta, \phi, \theta_s, \phi_s) = \frac{1}{2}(1+\cos(\theta)^2)\left[\frac{1}{MN}\left(1 + e^{j(\psi_y/2+\psi_x)}\right)\frac{\sin((M/2)\psi_x)}{\sin(\psi_x)}\frac{\sin((N/2)\psi_x)}{\sin(\psi_x/2)}\right]^2, \tag{9}$$

where $\psi_x = -kd_x(\sin\theta\cos\phi - \sin\theta_s\cos\phi_s)$, $\psi_y = -kd_y(\sin\theta\sin\phi - \sin\theta_s\sin\phi_s)$.

This spatial ambiguity is a separable function made up of the components of $W(\tau, r)$ and $F(\theta, \phi, \theta_s, \phi_s)$. These two functions can be combined by multiplying, creating the spatial ambiguity function $K(\tau, \mathbf{r}_s, \mathbf{r})$, and then doing a volume integration. This will create radar system's estimate of the ACF which will be referred to as $\rho(\tau, \mathbf{r}_s)$,

$$\rho(\tau, \mathbf{r}_s) = \int F(\theta, \phi, \theta_s, \phi_s)W(\tau, r_s, r)R(\tau, \mathbf{r})dV, \tag{10}$$

$$= \int K(\tau, \mathbf{r}_s, \mathbf{r})R(\tau, \mathbf{r})dV. \tag{11}$$

A rendering of an example of this full ambiguity function for an uncoded long pulse and antenna pattern in (9) for four beams can be seen in Figure 1.

Lastly, since the radar requires a finite amount of time to average pulses to create the estimate of the ACF we will add slow-time dependence to R. We will add another separable function $G(t_s, t)$ to the kernel,

$$\rho(\tau, \mathbf{r}_s, t_s) = \int G(t_s, t) K(\tau, \mathbf{r}_s, \mathbf{r}) R(\tau, \mathbf{r}, t) dV dt \tag{12}$$

$$\rho(\tau, \mathbf{r}_s, t_s) = \int L(\tau, \mathbf{r}_s, t_s, \mathbf{r}, t) R(\tau, \mathbf{r}, t) dV dt. \tag{13}$$

The final kernel, $L(\tau, \mathbf{r}_s, t_s, \mathbf{r}, t)$ encompasses the full space-time ambiguity.

2.2. Ambiguity after Frame Transformation

We will now focus on the impact of the motion of plasma as it is going through the field of view of the radar. We will assume that the radar is integrating over a length of time T beginning at t_s. The kernel L will be represented as a separable function K and G as in (12). In this case G will be an indicator function of length T and centered at $t_0 + 1/2$. This will change (12) to the following,

$$\rho(\tau, \mathbf{r}_s, t_s) = \int K(\tau, \mathbf{r}_s, \mathbf{r}) \int_{t_s}^{t_s+T} R(\tau, \mathbf{r}, t) dt dV. \tag{14}$$

At this point it will be assumed that the plasma is rigid object and will not deform with respect to $\mathbf{r}$ over time period $[t_0, t_0 + T]$. Also it will be assumed that it will be moving with a constant velocity $\mathbf{v}$. Thus $R(\tau, \mathbf{r}, t) \Rightarrow R(\tau, \mathbf{r} + \mathbf{v}t)$. At this point (14) becomes,

$$\rho(\tau, \mathbf{r}_s, t_s) = \int \int_{t_s}^{t_s+T} K(\tau, \mathbf{r}_s, \mathbf{r}) R(\tau, \mathbf{r} + \mathbf{v}t) dt dV \tag{15}$$

153 A change of variables where $\mathbf{r}' = \mathbf{r} + \mathbf{v}t$ acts as a Galilean transform and applies a
154 warping to the kernel and changing the frame of reference. Then (15) becomes

$$\rho(\tau, \mathbf{r}_s, t_s) = \int \int_{t_s}^{t_s+T} K(\tau, \mathbf{r}_s, \mathbf{r}' - \mathbf{v}t) R(\tau, \mathbf{r}') dt dV. \tag{16}$$

155 Since $R(\tau, \mathbf{r}')$ is no longer dependent on t (16) becomes,

$$\rho(\tau, \mathbf{r}_s, t_s) = \int \left[\int_{t_s}^{t_s+T} K(\tau, \mathbf{r}_s, \mathbf{r}' - \mathbf{v}t) dt \right] R(\tau, \mathbf{r}') dV. \tag{17}$$

156 By performing the integration in t the problem can now be simplified further back
157 to a Fredholm integral equation by simply replacing the terms in the square brackets
158 as a new kernel A,

$$\rho(\tau, \mathbf{r}_s, t_s) = \int A(\tau, \mathbf{r}_s, t_s, \mathbf{r}') R(\tau, \mathbf{r}') dV. \tag{18}$$

159 The impact of the plasma velocity on the ambiguity function can be seen in Figure
160 2. This is the same ambiguity as seen in Figure 1 but with a velocity of 500 m/s in
161 the y direction over a period of 2 minutes. This velocity creates a larger ambiguity
162 function in the frame of reference of the moving plasma.

163 The operator A can be determined through knowledge of the radar system's beam
164 pattern along with the experiments pulse pattern, integration time and velocity of
165 the plasma. This velocity $\mathbf{v}$ can be estimated by taking taking measurements of the

Doppler shift and using a methodology seen in *Butler et al.* [2010]. Once the operator has been determined standard processing techniques can be used as if the plasma is not moving.

3. Simulation

In order to determine if it is possible to improve the resolution of ISR processing synthetic data was created using a known condition of a simulated ionosphere. The simulator creates data by deriving filters from the autocorrelation function and applying it to complex white Gaussian noise. In a sense every point in time and space noise plant and filter structure as in Figure 3. The data is then scaled and summed together according to its location in range and angle space to radar.

To test this a phantom ionosphere is created where a small plasma enhancement moves through the radar field of view. The background electron density varies in altitude as a Chapman function while the electron and ion temperature remains constant. This is done to avoid having to do full fit and thus only try to measure the electron density. Also estimates of the zeroth lag are only necessary. Added to this is a 35 km radius sphere of enhance electron density of about 5×10^{10} m^{-3} centered at 400 km altitude moving at 500 m/s along the y direction.

4. Possible Mitigation Techniques

There are a number of possible ways to remove the ISR operator function to the data. A relatively simply way to remove the problem is to process the data in the frame of reference of the plasma. This technique includes measuring the ion velocity

185 of the plasma and then integrating the beams that the plasma is present in as it
186 moves through the field of view.

5. Conclusion

References

187 (2005), Eiscat 3d design specification document.

188 (2014), Amisr overview.

189 Balanis, C. A. (2005), *Antenna Theory: Analysis and Design*, Wiley-Interscience.

190 Butler, T. W. (2013), Spatial statistics and analysis of Earth's ionosphere, Ph.D.
191 thesis.

192 Butler, T. W., J. Semeter, C. J. Heinselman, and M. J. Nicolls (2010), Imaging f
193 region drifts using monostatic phased-array incoherent scatter radar, *Radio Sci.*,
194 *45*(5), RS5013, doi:10.1029/2010RS004364.

195 Dahlgren, H., J. L. Semeter, K. Hosokawa, M. J. Nicolls, T. W. Butler, M. G. Johnsen,
196 K. Shiokawa, and C. Heinselman (2012a), Direct three-dimensional imaging of polar
197 ionospheric structures with the resolute bay incoherent scatter radar, *Geophysical*
198 *Research Letters*, *39*(5), n/a–n/a, doi:10.1029/2012GL050895.

199 Dahlgren, H., G. W. Perry, J. L. Semeter, J. P. St. Maurice, K. Hosokawa,
200 M. J. Nicolls, M. Greffen, K. Shiokawa, and C. Heinselman (2012b), Space-
201 time variability of polar cap patches: Direct evidence for internal plasma struc-
202 turing, *Journal of Geophysical Research: Space Physics*, *117*(A9), A09,312, doi:
203 10.1029/2012JA017961.

Dougherty, J. P., and D. T. Farley (1960), A theory of incoherent scattering of radio waves by a plasma, *Proceedings of the Royal Society of London. Series A, Mathematical and Physical Sciences*, *259*(1296), pp. 79–99.

Dougherty, J. P., and D. T. Farley (1963), A theory of incoherent scattering of radio waves by a plasma, 3 scattering in a partly ionized gas, *Journal of Geophysical Research*, *68*, 5473.

Farley, D. T., J. P. Dougherty, and D. W. Barron (1961), A theory of incoherent scattering of radio waves by a plasma ii. scattering in a magnetic field, *Proceedings of the Royal Society of London. Series A, Mathematical and Physical Sciences*, *263*(1313), pp. 238–258.

Gordon, W. (1958), Incoherent scattering of radio waves by free electrons with applications to space exploration by radar, *Proceedings of the IRE*, *46*(11), 1824–1829, doi:10.1109/JRPROC.1958.286852.

Hagfors, T. (1961), Density fluctuations in a plasma in a magnetic field, with applications to the ionosphere, *Journal of Geophysical Research*, *66*(6), 1699–1712, doi:10.1029/JZ066i006p01699.

Holt, J. M., D. A. Rhoda, D. Tetenbaum, and A. P. van Eyken (1992), Optimal analysis of incoherent scatter radar data, *Radio Sci.*, *27*(3), 435–447, doi:10.1029/91RS02922.

Hysell, D. L., F. S. Rodrigues, J. L. Chau, and J. D. Huba (2008), Full profile incoherent scatter analysis at jicamarca, *Annales Geophysicae*, *26*(1), 59–75, doi:10.5194/angeo-26-59-2008.

Kudeki, E. (2003), *ECE 458 Lecture Notes, Application to Radio Wave Propagation*, Univ. Of Illinois, Urbana IL.

Lehtinen, M. S. (1989), On optimization of incoherent scatter measurements, *Advances in Space Research*, *9*(5), 133 – 141, doi:http://dx.doi.org/10.1016/0273-1177(89)90351-7.

Lehtinen, M. S., and A. Huuskonen (1996), General incoherent scatter analysis and {GUISDAP}, *Journal of Atmospheric and Terrestrial Physics*, *58*(1–4), 435 – 452, doi:http://dx.doi.org/10.1016/0021-9169(95)00047-X, ¡ce:title¿Selected papers from the sixth international Eiscat Workshop¡/ce:title¿.

Lehtinen, M. S., A. Huuskonen, and J. Pirttilä (1997), First experiences of full-profile analysis with GUISDAP, *Annales Geophysicae*.

Nicolls, M. J., and C. J. Heinselman (2007), Three-dimensional measurements of traveling ionospheric disturbances with the Poker Flat Incoherent Scatter Radar, *Geophysical Research Letters*.

Nikoukar, R. (2010), Near-optimal inversion of incoherent scatter radar measurements- coding schemes, processing techniques, and experiments, Ph.D. thesis, University of Illinois at Urbana-Champaign.

Nikoukar, R., F. Kamalabadi, E. Kudeki, and M. Sulzer (2008), An efficient near-optimal approach to incoherent scatter radar parameter estimation, *Radio Science*, *43*(5), n/a–n/a, doi:10.1029/2007RS003724.

Richards, M. A. (2005), *Fundamentals of Radar Signal Processing*, McGraw-Hill.

Semeter, J., T. Butler, C. Heinselman, M. Nicolls, J. Kelly, and D. Hampton (2009), Volumetric imaging of the auroral ionosphere: Initial results from pfisr, *Journal of Atmospheric and Solar-Terrestrial Physics*, *71*, 738 – 743, doi: 10.1016/j.jastp.2008.08.014, ¡ce:title¿Advances in high latitude upper atmospheric science with the Poker Flat Incoherent Scatter Radar (PFISR)¡/ce:title¿.

Acknowledgments. (Text here)

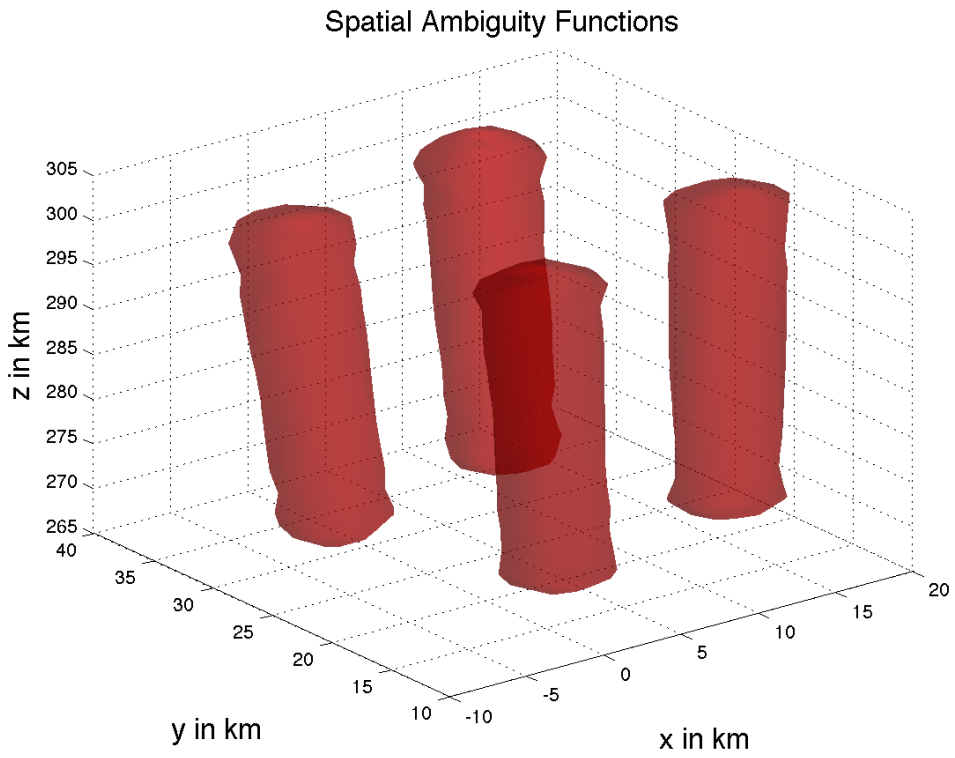

Figure 1. Full Spatial Ambiguity Function

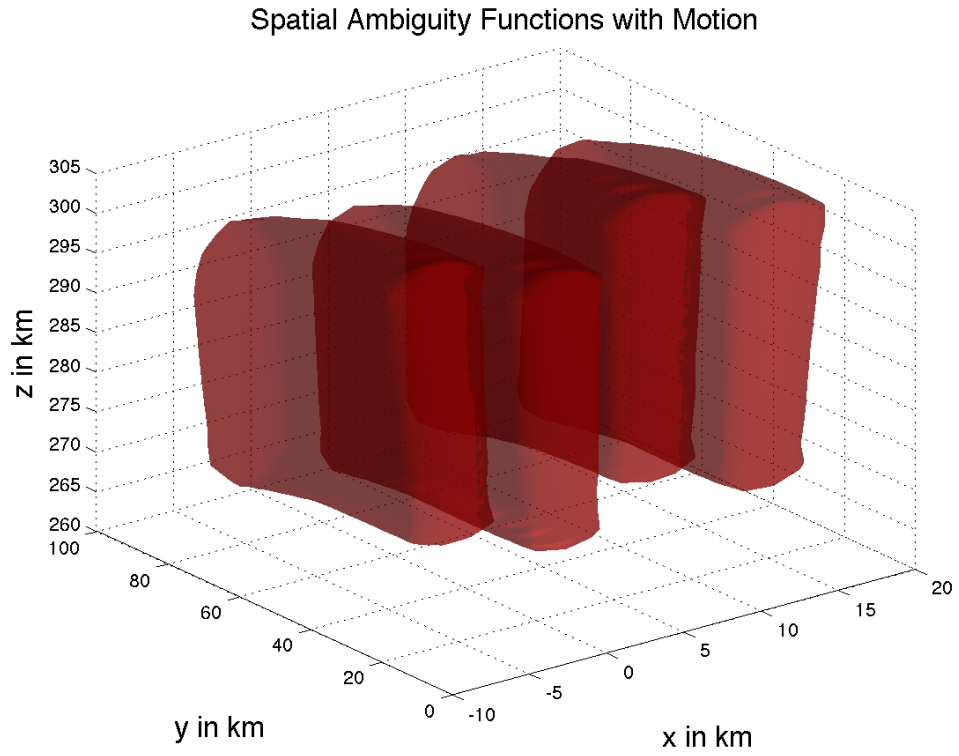

Figure 2. Full Spatial Ambiguity Function With Motion

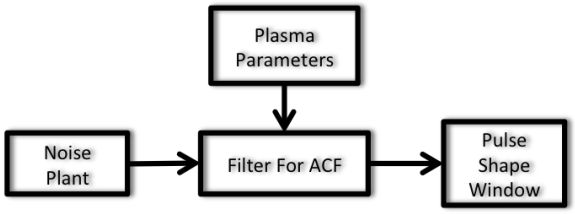

Figure 3. I/Q Simulator Diagram